(13) J. M. Haschke and H. A. Eick, *J. Am. Chem. Soc.*, **92**, 1526 (1970).
(14) J. M. Haschke, *Inorg. Chem.*, **14**, 779 (1975).
(15) K.-F. Seifert, *Fortschr. Mineral.*, **45**, 214 (1968).
(16) H. Baernighausen, H. P. Beck, and H.-W. Grueninger, *Proc. Rare Earth Res. Conf., 9th*, **1**, 74 (1971).
(17) H. Baernighausen, *Rev. Chim. Miner.*, **10**, 77 (1973).
(18) M. J. Buerger, *J. Chem. Phys.*, **15**, 1 (1947).
(19) J. Neubueser and H. Wondratschek, *Krist. Tech.*, **1**, 529 (1966).
(20) J. Neubueser and H. Wondratschek "Maximal Subgroups and Minimal Supergroups of the Space Groups", private communication with H. Wondratschek, University of Karlsruhe, Karlsruhe, West Germany, 1974.
(21) D. Brown, "Halides of the Lanthanides and Actinides", Wiley, New York, N.Y., 1968.
(22) J. D. Corbett, *Rev. Chim. Miner.*, **10**, 239 (1973).
(23) L. F. Druding, J. D. Corbett, and N. B. Ramsey, *Inorg. Chem.*, **2**, 869 (1963).
(24) G. I. Novikov and O. G. Polyachenok, *Zh. Neorg. Khim.*, **8**, 1053 (1963); *Russ. J. Inorg. Chem.*, **8**, 545 (1963).
(25) L. F. Druding and J. D. Corbett, *J. Am. Chem. Soc.*, **83**, 2462 (1961).
(26) N. A. Fishel and H. A. Eick, *J. Inorg. Nucl. Chem.*, **33**, 1201 (1971).
(27) O. G. Polyachenok and G. I. Novikov, *Zh. Neorg. Khim.*, **8**, 2818 (1963); *Russ. J. Inorg. Chem.*, **8**, 1478 (1963).
(28) U. Loechner and J. D. Corbett, *Inorg. Chem.*, **14**, 426 (1975).
(29) J. D. Corbett and B. C. McCollum, *Inorg. Chem.*, **5**, 938 (1966).
(30) P. E. Caro and J. D. Corbett, *J. Less-Common Met.*, **18**, 1 (1969).
(31) J. D. Corbett, L. F. Druding, W. J. Burkhard, and C. B. Lindahl, *Discuss. Faraday Soc.*, **32**, 79 (1961).
(32) R. A. Sallach and J. D. Corbett, *Inorg. Chem.*, **2**, 457 (1963).
(33) J. D. M. Bevan in "Comprehensive Inorganic Chemistry", Vol. 4, J. C. Bailar, Jr., H. J. Emeleus, R. Nyholm, and A. F. Trotman-Dickenson Ed., Pergamon Press, Oxford, 1973, Chapter 49.
(34) J. M. Haschke, *J. Solid State Chem.*, **14**, 238 (1975).
(35) A. N. Christensen, *Acta Chem. Scand.*, **19**, 1391 (1965).
(36) A. F. Wells, "Structural Inorganic Chemistry", 3rd ed, Oxford University Press, London, 1962, Chapter XXVI.
(37) B. G. Hyde, A. N. Bagshaw, S. Anderson, and M. O'Keeffe, *Annu. Rev. Mater. Sci.*, **4**, 43–92 (1974).
(38) P. E. Caro, *Natl. Bur. Stand. (U.S.), Spec. Publ.*, **No. 364**, 367 (1972).

Contribution from the Department of Chemistry, University of Canterbury, Christchurch, New Zealand

Crystal Structures of the Pentakis(trimethylarsine oxide)metal(II) Perchlorates [Ni(Me3AsO)5](ClO4)2 and [Mg(Me3AsO)5](ClO4)2

Y. S. NG, G. A. RODLEY,* and WARD T. ROBINSON

Received March 13, 1975 AIC50189H

The crystal structures of two isomorphous compounds, pentakis(trimethylarsine oxide)nickel(II) perchlorate, [Ni(Me3AsO)5](ClO4)2, and its magnesium analogue, have been determined by x-ray analyses. The compounds crystallize in the centrosymmetric space group $P2_1/n$, with four molecules in unit cells of dimensions a = 11.301 (3), 11.330 (5) Å, b = 27.256 (6), 27.562 (6) Å, c = 11.294 (5), 11.328 (6) Å, and β = 90.41 (3), 90.58 (5)° for the nickel and magnesium complexes, respectively. The structures were solved using diffractometer data and difference Patterson techniques. Least-squares refinements converged with final conventional R values of 0.064 (3975 data) and 0.068 (3552 data) for the nickel and magnesium complexes, respectively. The structures consist of discrete $[M(Me_3AsO)_5]^{2+}$ (M = Ni, Mg) cations well separated from perchlorate anions. The coordination geometry around the metal atoms is approximately square pyramidal, with nickel and magnesium atoms 0.359 (3) and 0.454 (3) Å above the least-squares plane of the basal oxygen and arsenic atoms, respectively. The arrangements of atoms around the central metal atoms are discussed in terms of the different electronic properties of magnesium and nickel. Small but significant differences between the two structures indicate the binding of the Me3AsO ligands is more than simple σ donation. Other structural features, notably a large cavity in the coordination sphere, also indicate that electronic rather than steric factors govern the structures of the cations.

Introduction

It is now apparent that monodentate oxo ligands of the type R_3XO (X = P, As) readily form five-coordinate complexes with metal(II) perchlorates.[1-7] Two basic types are obtained: $[M(R_3XO)_4ClO_4](ClO_4)^2$ and $[M(R_3XO)_5](ClO_4)_2$.[8] Preliminary x-ray photographic studies of $[Co(Ph_2MeAsO)_4ClO_4]ClO_4$ and $[Ni(Me_3AsO)_5](ClO_4)_2$ have shown the cations have essentially the same square-pyramidal structures.[2,8] We have now completed detailed analyses of the latter complex and its magnesium analogue using accurate diffractometer data sets.

The present results enable us to reassess the reasons for the formation of the square-pyramidal geometry in such systems. Previously attention was focused on steric factors. We now believe electronic binding properties of the oxo ligands are of prime importance. Also small but significant differences between the nickel and magnesium structures give further insight into the bonding of oxo ligands to metal ions.

Formation of five-coordinate complexes by non transition metal ions such as calcium and magnesium has not been studied extensively. However this geometry could be of considerable importance in biological systems.

While octahedral coordination may be the most common geometry for these ions, ligand systems with appropriate properties (electronic as well as steric) readily produce five-coordinate Ca^{2+} and Mg^{2+} complexes. The magnesium structure reported here provides detailed information on a magnesium complex, representative of a range of five-coordinate complexes of Ca^{2+} and Mg^{2+} recently prepared with oxo ligands.[9] A basically similar square-pyramidal structure has been found from an x-ray analysis of a chlorophyll-like aquomagnesium tetraphenylporphyrin.[10] Also a five-coordinate structure for certain chlorophyll systems has been indicated from infrared and NMR studies.[11] In other biological systems hydrophobic regions of protein structures may facilitate coordination numbers less than 6 through the elimination of water from the coordination sphere.

Experimental Section

Orange, plate-shaped crystals of $[Ni(Me_3AsO)_5](ClO_4)_2$ were grown from an acetonitrile solution in the presence of an ether vapor.[12] Colorless, transparent, plate-shaped crystals of $[Mg(Me_3AsO)_5](ClO_4)_2$ were provided by Mr. G. B. Jameson.[9] The nickel crystals, being sensitive to moisture, were sealed in capillary tubes under a stream of nitrogen. The crystals were assigned to the monoclinic system after examination by Weissenberg and precession photography, using Cu Kα radiation. Conditions limiting possible reflections were uniquely consistent with the monoclinic space group $P2_1/c$ but it was found convenient to solve both structures using the unconventional setting $P2_1/n$ (equivalent positions: x, y, z; $-x, -y, -z$; $1/2 + x, 1/2 - y, 1/2 + z$; $1/2 - x, 1/2 + y, 1/2 - z$). All data in this paper refer to this latter space group setting.

Unit cell parameters were obtained by least-squares analysis of the setting angles of 12 reflections accurately centered in a 5.0-mm

Table I. Crystal Data

	$[Ni(Me_3AsO)_5](ClO_4)_2$	$[Mg(Me_3AsO)_5](ClO_4)_2$
Formula wt	937.74	903.34
a/Å	11.301 (3)	11.330 (5)
b/Å	27.256 (6)	27.562 (6)
c/Å	11.294 (5)	11.328 (6)
β/deg	90.41 (3)	90.58 (5)
V_c/Å^3	3478.8	3537.5
d_{measd}/g cm^{-3}		1.73
d_{calcd}/g cm^{-3}	1.79	1.70
Z	4	4
Max crystal dimension/mm	0.5	0.43
Min crystal dimension/mm	0.13	0.18

diameter collimator with its circular receiving aperture set at 230 mm from the crystal on a Hilger and Watts four-circle computer-controlled diffractometer (24°). Important crystal data are summarized in Table I. The figures in parentheses in Table I and elsewhere in this paper are estimated standard deviations in the least significant figures quoted and were usually derived from the inverse matrix in the course of normal least-squares refinement calculations.

The density of the nickel complex was not measured because of its sensitivity to moisture. However, the density of the magnesium complex was determined by flotation in a mixture of bromobenzene and dibromoethane.[13] This value agrees satisfactorily with the calculated density for 4 molecules in the unit cell. No crystallographic symmetry is imposed on individual molecules.

Collection and Reduction of Intensity Data

Data were collected using well-formed plate-shaped crystals. The boundary faces were identified and their distances from arbitrary origins in the crystals measured using a binocular microscope.

The mosaicity of each crystal was examined by means of open-counter ω scans at a takeoff angle of 3°. Intensities were collected using Zr-filtered Mo Kα x radiation for the Ni^{2+} complex whereas Ni-filtered Cu Kα x radiation was used for the Mg^{2+} complex. The intensities of all reflections were recorded using the θ–2θ scan techniques. Calibrated attenuators were used to bring strong reflections within the linear response range of the scintillation counter whenever counting rates exceeded 8000 counts/sec.

Throughout the data collection, three standard reflections were referred to regularly. These reflections dropped to 63% of their initial values in the case of the nickel complex. All reflections were adjusted to the same relative scale. No great fluctuations in the standard reflections occurred for the magnesium complex.

The standard deviation for each measured intensity was

$$\sigma(I) = [C + 0.25(t_c/t_b)^2(B_1 + B_2) + (pI)^2]^{1/2}$$

where C is the scan count, t_c and t_b are scan and background times, B_1 and B_2 are the background counts, p is assigned a value of 0.05 and is a factor used to avoid overweighting more intense reflections, and I was obtained from

$$I = C - 0.5(t_c/t_b)(B_1 + B_2)$$

Data were corrected for Lorentz–polarization effects and then for absorption[14] in the two compounds. Data collection and processing details are summarized in Table II.

Solution and Refinement of the Structures

In all least-squares refinements, the function minimized[15] was $\sum w(|F_o| - |F_c|)^2$, where w is assigned as $4F_o^2/\sigma(F_o^2)^2$, and $|F_o|$ and $|F_c|$ are the observed and calculated structure factor amplitudes respectively. Atomic scattering factors for nonhydrogen atoms were obtained from Cromer and Mann[16] and those for hydrogen atoms were from Stewart et al.[17] The real and imaginary contributions of anomalous scattering, $\Delta f'$ and $\Delta f''$, for As, Ni, Cl, and Mg were from Cromer's tabulation.[18] The conventional R factors are defined as

$$R_1 = \Sigma||F_o| - |F_c||/\Sigma|F_o|$$

$$R_2 = (\Sigma w(|F_o| - |F_c|)^2/\Sigma w|F_o|^2)^{1/2}$$

The original structure analysis, using film data and symbolic addition procedures, had converged with an R factor of 0.13 (1171 data).[8] However, these atom parameters did not lead to satisfactory refinements with the new diffractometer data sets and were abandoned. The positions of the central metal atom and the five arsenic atoms were then obtained from the difference between Patterson syntheses calculated using the diffractometer data sets.[19] Both of the unsharpened Patterson maps for the Ni^{2+} and Mg^{2+} complexes were placed on the same relative scale by equating average, dominant, equivalent As–As vector peak densities. The map for the magnesium complex was subtracted from that of the nickel. An image of a square-pyramidal arrangement of five arsenic atoms about one metal atom was located with the metal atom centered at the origin. A similar arrangement, presumed related by a twofold screw axis, was also discerned and served to position these atoms absolutely in real space. Full-matrix least-squares refinements of positional and isotropic thermal parameters for these six atoms, using data from the magnesium complex, led to values of 0.366 and 0.445 for R_1 and R_2, respectively. A difference Fourier synthesis showed the locations of all the nonhydrogen atoms in the structure except the apical methyl carbon atoms of the cation and the oxygen atoms of the perchlorate anions. The remaining atoms were found from successive structure factor calculations and difference Fourier syntheses. Refinements were carried out using isotropic temperature factors and this model gave $R_1 = 0.120$ and $R_2 = 0.160$. The same positional parameters and isotropic temperature factors were transferred to the nickel complex and refined to convergence with $R_1 = 0.120$ and $R_2 = 0.137$, respectively. A difference Fourier synthesis at this stage showed considerable anisotropic thermal motion for most atoms in the structure. Core storage limitations of our computer permitted only 176 parameters to be varied simultaneously. Therefore, least-squares refinements using anisotropic temperature factors were carried out in two separate blocks for each structure. The scale factor and all parameters for the nickel and axial arsenic atoms were varied in both blocks. The parameters for the perchlorate anions, the four basal arsenic atoms, and the axial ligand carbon atoms were varied in the first block. The parameters for all of the arsine oxide oxygen and basal methyl carbon atoms were varied in the second block. These refinements converged with $R_1 = 0.064$ and $R_2 = 0.076$ for the nickel structure and $R_1 = 0.068$ and $R_2 = 0.083$ for the magnesium structure. These low R factors and the extremely close similarity of the two structures are taken to indicate that both refined models are correct. However two of the methyl carbons, in the Ni^{2+} complex only, C(22) and C(42) had non-positive-definite temperature factors indicating that the thermal ellipsoid representation for these two atoms was not physically reasonable. Shifts in the last cycles of refinements were all less than 1.1 and 0.8 of the estimated standard deviations for the nickel and magnesium complex parameters, respectively.

Final difference Fourier syntheses showed no peaks higher than those assigned to highly anisotropic methyl carbon atoms in earlier such calculations. Examinations of average values of the minimized function over ranges of $|F_o|$ and $\lambda^{-1}\sin\theta$ showed the weighting schemes chosen were satisfactory. The standard errors in observations of unit weight are 1.99 and 2.33 for the nickel and magnesium complexes, respectively.

Final positional and anisotropic thermal parameters are listed in Tables III and IV. Comparison of these values with those obtained in the earlier analysis[8] showed that, although the published cationic

Table II. Experimental Parameters

	$[Ni(Me_3AsO)_5](ClO_4)_2$	$[Mg(Me_3AsO)_5](ClO_4)_2$
Mosaicity/deg	0.19	0.18
θ-Scan range/deg	0.72	0.90
Scan time/sec	72	90
Total background time/sec	18	22.5
θ limit/deg	22	50
Total independent reflections	3975	3552
Reflections used in refinement for which $\|F\|^2 \geq 3\sigma(\|F\|^2)$	1890	2413
Range of transmission factors	0.31–0.50	0.04–0.03
Weighting parameter p	0.05	0.05
Primary beam collimator diameter/mm	2.0	2.0
Secondary beam collimator diameter/mm	5.0	5.0

Table III. Positional and Thermal Parameters for $[Ni(Me_3AsO)_5](ClO_4)_2$

Atom	x	y	z	U_{11}[a]	U_{22}	U_{33}	U_{12}	U_{13}	U_{23}
Ni	0.0920 (3)	0.1085 (1)	0.1382 (2)	0.031 (2)	0.055 (2)	0.029 (2)	−0.001 (2)	0.004 (2)	−0.002 (2)
As(1)	0.2558 (2)	0.0999 (1)	−0.0977 (2)	0.034 (2)	0.075 (2)	0.035 (2)	−0.002 (2)	0.009 (2)	−0.004 (2)
As(2)	0.3268 (2)	0.0894 (1)	0.3056 (2)	0.038 (2)	0.087 (3)	0.036 (2)	0.002 (2)	−0.004 (2)	0.002 (2)
As(3)	−0.0777 (2)	0.1008 (1)	0.3732 (2)	0.040 (2)	0.089 (2)	0.035 (2)	0.001 (2)	0.006 (2)	0.002 (2)
As(4)	−0.1443 (2)	0.0958 (1)	−0.0288 (2)	0.035 (2)	0.083 (2)	0.032 (2)	−0.003 (2)	−0.002 (2)	−0.002 (2)
As(5)	0.0897 (3)	0.2366 (1)	0.1484 (2)	0.079 (3)	0.056 (2)	0.069 (2)	0.000 (2)	0.009 (2)	0.003 (2)
O(1)	0.125 (1)	0.0914 (5)	−0.031 (1)	0.04 (2)	0.11 (2)	0.038 (9)	0.01 (1)	0.005 (8)	−0.001 (9)
O(2)	0.257 (1)	0.0865 (5)	0.175 (1)	0.008 (9)	0.09 (2)	0.047 (9)	0.010 (8)	0.003 (7)	0.012 (8)
O(3)	0.054 (1)	0.1042 (6)	0.311 (1)	0.04 (2)	0.13 (2)	0.035 (9)	0.02 (2)	0.016 (8)	0.010 (9)
O(4)	−0.079 (1)	0.0950 (6)	0.103 (1)	0.03 (2)	0.10 (2)	0.06 (1)	0.007 (9)	−0.004 (9)	0.002 (9)
O(5)	0.112 (2)	0.1787 (6)	0.121 (1)	0.16 (3)	0.08 (2)	0.09 (2)	0.02 (2)	0.01 (2)	−0.00 (2)
C(11)	0.352 (2)	0.0418 (9)	−0.076 (2)	0.08 (3)	0.09 (3)	0.08 (2)	0.02 (2)	0.01 (2)	−0.00 (2)
C(12)	0.227 (2)	0.1052 (9)	−0.265 (2)	0.06 (2)	0.13 (3)	0.02 (2)	0.02 (2)	−0.01 (2)	0.00 (2)
C(13)	0.338 (2)	0.1572 (9)	−0.055 (2)	0.06 (2)	0.08 (2)	0.09 (2)	−0.03 (2)	0.04 (2)	−0.00 (2)
C(21)	0.265 (2)	0.0394 (8)	0.412 (2)	0.08 (3)	0.06 (2)	0.07 (2)	0.01 (2)	−0.01 (2)	0.03 (2)
C(22)	0.491 (2)	0.074 (1)	0.271 (2)	0.00 (2)	0.27 (4)	0.08 (2)	0.02 (2)	−0.00 (2)	−0.03 (3)
C(23)	0.314 (3)	0.1514 (9)	0.378 (2)	0.11 (3)	0.07 (3)	0.10 (3)	−0.02 (2)	−0.03 (2)	0.00 (2)
C(31)	−0.156 (2)	0.0383 (9)	0.336 (2)	0.10 (3)	0.07 (3)	0.10 (3)	0.00 (2)	0.02 (2)	−0.04 (2)
C(32)	−0.054 (2)	0.103 (1)	0.541 (2)	0.10 (3)	0.15 (3)	0.02 (2)	−0.00 (2)	−0.00 (2)	0.01 (2)
C(33)	−0.186 (3)	0.154 (1)	0.330 (2)	0.09 (3)	0.09 (3)	0.10 (3)	−0.04 (2)	0.02 (2)	0.02 (2)
C(41)	−0.113 (2)	0.0367 (8)	−0.116 (2)	0.06 (3)	0.06 (2)	0.08 (2)	−0.01 (2)	0.00 (2)	0.03 (2)
C(42)	−0.315 (2)	0.0996 (9)	0.004 (2)	−0.00 (2)	0.15 (3)	0.07 (2)	−0.01 (2)	−0.01 (2)	−0.01 (2)
C(43)	−0.104 (2)	0.1532 (9)	−0.125 (2)	0.10 (3)	0.09 (2)	0.05 (2)	−0.01 (2)	0.00 (2)	−0.03 (2)
C(51)	0.084 (4)	0.251 (1)	0.315 (2)	0.31 (6)	0.13 (4)	0.08 (3)	0.05 (4)	0.01 (3)	−0.04 (3)
C(52)	−0.056 (3)	0.261 (1)	0.086 (3)	0.12 (4)	0.15 (4)	0.24 (5)	−0.10 (3)	−0.07 (4)	0.01 (4)
C(53)	0.198 (3)	0.274 (1)	0.062 (4)	0.13 (4)	0.05 (3)	0.33 (6)	−0.02 (3)	0.08 (4)	0.02 (3)
Cl(1)	0.0792 (8)	0.4108 (3)	0.1499 (7)	0.058 (6)	0.083 (6)	0.067 (5)	−0.001 (6)	0.003 (5)	0.006 (5)
Cl(2)	0.085 (1)	0.2537 (4)	−0.3255 (9)	0.114 (9)	0.089 (8)	0.121 (9)	−0.008 (7)	−0.005 (8)	0.002 (6)
O(11)	0.025 (3)	0.3749 (8)	0.206 (2)	0.23 (4)	0.08 (2)	0.25 (3)	−0.05 (2)	0.12 (3)	−0.01 (2)
O(12)	0.131 (3)	0.405 (1)	0.047 (2)	0.20 (4)	0.29 (4)	0.14 (3)	0.07 (3)	0.09 (3)	−0.01 (3)
O(13)	0.161 (3)	0.428 (1)	0.210 (2)	0.30 (5)	0.45 (6)	0.15 (3)	−0.25 (5)	−0.18 (3)	0.14 (3)
O(14)	0.000 (3)	0.446 (1)	0.138 (3)	0.17 (4)	0.18 (3)	0.32 (4)	0.07 (3)	0.14 (3)	0.11 (3)
O(21)	0.046 (4)	0.220 (1)	−0.396 (3)	0.34 (6)	0.14 (3)	0.31 (5)	−0.08 (3)	0.02 (4)	−0.09 (3)
O(22)	0.158 (3)	0.236 (1)	−0.237 (3)	0.20 (4)	0.22 (3)	0.21 (3)	0.02 (3)	−0.10 (3)	0.07 (3)
O(23)	−0.000 (4)	0.274 (2)	−0.270 (4)	0.24 (6)	0.48 (8)	0.39 (7)	0.20 (6)	0.05 (5)	−0.11 (6)
O(24)	0.141 (3)	0.287 (1)	−0.385 (3)	0.26 (5)	0.24 (5)	0.30 (5)	−0.13 (4)	−0.12 (4)	0.14 (4)

[a] The form of the thermal ellipsoid expression is $\exp[-(\beta_{11}h^2 + \beta_{22}k^2 + \beta_{33}l^2 + 2\beta_{12}hk + 2\beta_{13}hl + 2\beta_{23}kl)]$; $U_{ij} = \beta_{ij}/2\pi^2 a_i^* a_j^*$ (Å).

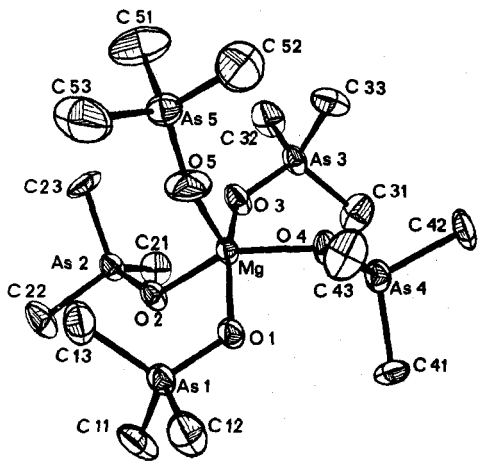

Figure 1. Perspective view of the $[Mg(Me_3AsO)_5]^{2+}$ cation showing 30% probability thermal ellipsoids.

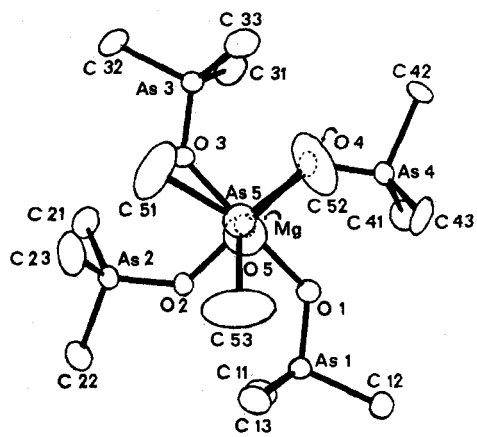

Figure 2. View of the $[Mg(Me_3AsO)_5]^{2+}$ cation looking down the crystallographic *b* axis.

structure was correct, the ions were incorrectly located in the unit cell.

Root-mean-square amplitudes of vibrations are given in Table V. Listings of final values of $|F_o|$ and $|F_c|$ (in electrons) for the reflections used in the refinements of both structures will appear following these pages in the microfilm edition of this journal (see paragraph at end of paper regarding supplementary material).

Description of the Crystal Structures

In the crystalline state, the two isomorphous compounds $[M(Me_3AsO)_5](ClO_4)_2$ (M = Ni, Mg) consist of well-separated ions, all interionic distances not involving hydrogen atoms being greater than 3.3 Å. Figure 1 is a perspective view of the $[Mg(Me_3AsO)_5]^{2+}$ cation and defines the atomic numbering scheme used throughout this paper for both complexes. Another view of the same ion is presented in Figure 2. Important interatomic distances and bond angles are collected in Tables VI and VII, respectively.

The perchlorate anions are well removed from the square-pyramidal cation. Although the anions have relatively high thermal motions, they exhibit no chemically significant deviations from normal tetrahedral geometry. The bond lengths and angles in the perchlorate anions range from 1.23 to 1.38 Å and from 101 to 123°. Their positions with respect to the cations are illustrated in the stereoscopic lattice packing diagram (Figure 3). The square base of the pyramid is parallel to the B face of the unit cell. Intercationic distances not involving hydrogen atoms are all greater than 3.5 Å in both structures. Disregarding the axial ligand methyl groups, the $[M(Me_3AsO)_5]^{2+}$ cation has approximate C_4 geometry. The

Table IV. Positional and Thermal Parameters for $[Mg(Me_3AsO)_5](ClO_4)_2$

Atom	x	y	z	U_{11}	U_{22}	U_{33}	U_{12}	U_{13}	U_{23}
Mg	0.0908 (3)	0.1112 (1)	0.1381 (4)	0.032 (3)	0.052 (3)	0.039 (3)	−0.000 (3)	−0.001 (2)	−0.000 (3)
As(1)	0.2552 (1)	0.1014 (1)	−0.1009 (1)	0.0418 (9)	0.077 (2)	0.042 (1)	−0.0037 (9)	0.0045 (8)	−0.0049 (9)
As(2)	0.3261 (1)	0.0876 (1)	0.3051 (1)	0.042 (1)	0.078 (2)	0.043 (2)	0.0043 (9)	−0.0043 (8)	−0.0003 (9)
As(3)	−0.0794 (1)	0.1001 (1)	0.3744 (1)	0.042 (1)	0.093 (2)	0.041 (2)	0.0007 (9)	0.0050 (8)	0.0036 (9)
As(4)	−0.1461 (1)	0.0934 (1)	−0.0299 (1)	0.0396 (9)	0.078 (2)	0.041 (1)	−0.0031 (9)	−0.0052 (8)	−0.0009 (9)
As(5)	0.0890 (2)	0.2394 (1)	0.1503 (2)	0.075 (2)	0.053 (1)	0.068 (2)	0.001 (1)	0.0021 (9)	0.0035 (9)
O(1)	0.1255 (7)	0.0947 (4)	−0.0345 (7)	0.039 (6)	0.095 (8)	0.043 (6)	−0.003 (6)	0.004 (5)	−0.018 (6)
O(2)	0.2539 (7)	0.0859 (3)	0.1759 (7)	0.038 (6)	0.090 (8)	0.041 (6)	0.008 (5)	−0.005 (5)	0.002 (6)
O(3)	0.0502 (8)	0.1025 (4)	0.3113 (8)	0.043 (6)	0.116 (9)	0.049 (7)	0.007 (6)	0.010 (5)	−0.001 (6)
O(4)	−0.0773 (7)	0.0923 (4)	0.1030 (7)	0.044 (6)	0.093 (8)	0.036 (6)	0.011 (6)	−0.011 (5)	−0.002 (5)
O(5)	0.105 (1)	0.1804 (4)	0.128 (1)	0.13 (2)	0.047 (7)	0.14 (2)	0.022 (8)	0.013 (9)	−0.007 (7)
C(11)	0.351 (1)	0.0458 (7)	−0.076 (2)	0.06 (2)	0.13 (2)	0.09 (2)	0.04 (2)	0.017 (9)	−0.00 (2)
C(12)	0.224 (1)	0.1080 (7)	−0.267 (1)	0.06 (2)	0.15 (2)	0.05 (2)	0.00 (2)	−0.000 (9)	0.01 (2)
C(13)	0.343 (1)	0.1574 (7)	−0.052 (1)	0.06 (2)	0.12 (2)	0.08 (2)	−0.02 (2)	0.007 (9)	−0.00 (2)
C(21)	0.270 (1)	0.0387 (6)	0.413 (1)	0.09 (2)	0.10 (2)	0.05 (1)	−0.01 (2)	−0.006 (9)	0.029 (9)
C(22)	0.490 (1)	0.0748 (8)	0.271 (1)	0.04 (1)	0.18 (3)	0.07 (2)	0.02 (2)	−0.011 (9)	−0.00 (2)
C(23)	0.313 (2)	0.1512 (5)	0.377 (1)	0.11 (2)	0.06 (2)	0.09 (2)	−0.00 (2)	−0.04 (2)	−0.04 (1)
C(31)	−0.157 (2)	0.0391 (7)	0.338 (2)	0.12 (2)	0.12 (2)	0.08 (2)	0.04 (2)	0.01 (2)	−0.01 (2)
C(32)	−0.056 (2)	0.1026 (9)	0.544 (1)	0.09 (2)	0.19 (3)	0.05 (2)	−0.00 (2)	0.019 (9)	0.01 (2)
C(33)	−0.182 (1)	0.1501 (6)	0.327 (1)	0.09 (2)	0.10 (2)	0.08 (2)	−0.03 (2)	0.02 (1)	0.01 (2)
C(41)	−0.110 (1)	0.0366 (6)	−0.117 (1)	0.08 (2)	0.09 (2)	0.07 (2)	−0.02 (1)	−0.014 (9)	0.05 (1)
C(42)	−0.315 (1)	0.0948 (7)	0.000 (1)	0.023 (8)	0.15 (2)	0.07 (2)	−0.000 (9)	0.001 (8)	0.01 (2)
C(43)	−0.108 (2)	0.1510 (6)	−0.121 (1)	0.12 (2)	0.09 (2)	0.04 (1)	0.02 (2)	−0.021 (9)	−0.040 (9)
C(51)	0.100 (2)	0.2586 (8)	0.311 (2)	0.25 (3)	0.11 (2)	0.07 (2)	0.02 (2)	−0.01 (2)	−0.02 (2)
C(52)	−0.057 (2)	0.2611 (9)	0.099 (3)	0.12 (2)	0.11 (2)	0.24 (3)	−0.05 (2)	−0.08 (2)	0.00 (2)
C(53)	0.207 (2)	0.2734 (8)	0.073 (3)	0.18 (3)	0.10 (2)	0.25 (4)	−0.00 (2)	0.13 (3)	0.01 (2)
Cl(1)	0.0783 (4)	0.4108 (2)	0.1484 (4)	0.061 (3)	0.078 (3)	0.074 (4)	−0.007 (3)	−0.000 (3)	0.003 (3)
Cl(2)	0.0787 (6)	0.2556 (2)	−0.3256 (6)	0.116 (5)	0.097 (4)	0.110 (5)	−0.003 (4)	−0.014 (4)	0.009 (4)
O(11)	0.033 (2)	0.3731 (6)	0.210 (2)	0.22 (2)	0.10 (2)	0.27 (3)	−0.07 (2)	0.12 (2)	−0.02 (2)
O(12)	0.121 (2)	0.403 (1)	0.041 (2)	0.38 (4)	0.34 (4)	0.09 (2)	0.13 (3)	0.07 (2)	0.01 (2)
O(13)	0.159 (2)	0.429 (1)	0.206 (2)	0.35 (4)	0.45 (5)	0.25 (3)	−0.29 (4)	−0.23 (3)	0.21 (3)
O(14)	−0.003 (2)	0.4463 (7)	0.139 (2)	0.15 (2)	0.18 (2)	0.38 (4)	0.08 (2)	0.12 (2)	0.12 (3)
O(21)	0.038 (3)	0.222 (1)	−0.398 (2)	0.36 (4)	0.21 (3)	0.23 (3)	−0.11 (3)	−0.03 (3)	−0.03 (3)
O(22)	0.153 (2)	0.2359 (8)	−0.244 (2)	0.26 (3)	0.20 (3)	0.25 (3)	0.02 (2)	−0.14 (3)	0.06 (2)
O(23)	−0.006 (3)	0.276 (2)	−0.266 (3)	0.33 (4)	0.55 (7)	0.25 (4)	0.26 (5)	0.06 (3)	−0.11 (4)
O(24)	0.132 (3)	0.290 (1)	−0.388 (2)	0.41 (5)	0.25 (3)	0.19 (3)	−0.16 (3)	−0.05 (3)	0.04 (3)

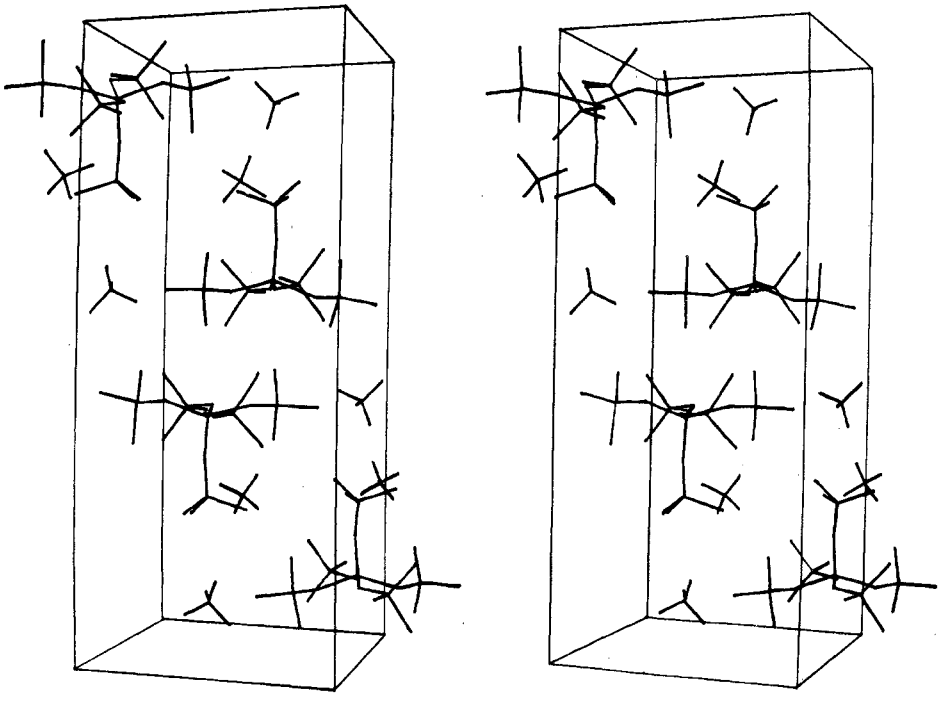

Figure 3. Stereogram showing contents of the unit cell of $[Mg(Me_3AsO)_5](ClO_4)_2$.

oxygen atoms O(1) to O(4), together with the arsenic atoms As(1) to As(4), though not statistically coplanar, are close to their best least-squares plane which is taken as the basal plane for a square pyramid. Table VIII defines these planes together with the displacements of selected atoms from them. The fifth axial oxygen atom does not lie directly above the central metal atom, being displaced approximately 0.1 Å from the normal vector of the basal plane in both complexes. However the apical arsenic atom is closely collinear with this normal vector; thus the arrangement of the arsenic atoms is also square pyramidal.

The M–O distances in the square pyramid range from 1.94 (2) to 2.01 (1) Å for M = Ni and from 1.92 (1) to 2.05 (1) Å for M = Mg. An interesting feature of the two complexes

Table V. Root-Mean-Square Amplitudes of Vibration (Å) for Selected Atoms

$[Ni(Me_3AsO)_5](ClO_4)_2$				$[Mg(Me_3AsO)_5](ClO_4)_2$			
Atom	Min	Intermed	Max	Atom	Min	Intermed	Max
Ni	0.162 (5)	0.182 (5)	0.234 (4)	Mg	0.178 (6)	0.200 (6)	0.229 (6)
As(1)	0.162 (4)	0.206 (4)	0.276 (3)	As(1)	0.194 (2)	0.212 (2)	0.279 (2)
As(2)	0.182 (4)	0.203 (4)	0.294 (4)	As(2)	0.194 (2)	0.217 (2)	0.280 (2)
As(3)	0.176 (4)	0.208 (4)	0.299 (3)	As(3)	0.192 (2)	0.214 (2)	0.305 (2)
As(4)	0.176 (4)	0.191 (4)	0.288 (3)	As(4)	0.186 (2)	0.215 (2)	0.279 (2)
As(5)	0.235 (4)	0.254 (4)	0.289 (4)	As(5)	0.229 (2)	0.261 (2)	0.274 (2)
O(1)	0.18 (3)	0.21 (2)	0.33 (2)	O(1)	0.19 (1)	0.20 (1)	0.32 (1)
O(2)	0.08 (5)	0.21 (2)	0.30 (2)	O(2)	0.18 (1)	0.21 (1)	0.30 (1)
O(3)	0.15 (3)	0.22 (2)	0.38 (2)	O(3)	0.19 (1)	0.24 (1)	0.34 (1)
O(4)	0.16 (3)	0.24 (2)	0.32 (2)	O(4)	0.17 (2)	0.22 (1)	0.31 (1)
O(5)	0.26 (3)	0.30 (2)	0.41 (3)	O(5)	0.20 (2)	0.36 (2)	0.38 (2)
C(51)	0.22 (5)	0.38 (4)	0.57 (5)	C(51)	0.24 (3)	0.34 (3)	0.51 (3)
C(52)	0.15 (7)	0.44 (5)	0.55 (5)	C(52)	0.23 (3)	0.37 (3)	0.53 (3)
C(53)	0.19 (5)	0.34 (5)	0.60 (4)	C(53)	0.28 (3)	0.32 (3)	0.58 (3)
Cl(1)	0.24 (1)	0.26 (1)	0.29 (1)	Cl(1)	0.241 (6)	0.270 (5)	0.286 (5)
Cl(2)	0.29 (1)	0.34 (1)	0.35 (1)	Cl(2)	0.303 (7)	0.318 (7)	0.362 (7)

is the significantly shorter axial, compared to basal, M–O bond. Comparisons between analogous bond angles reveal consistency to within 7.2° between cations in the two structures.

Discussion

The basically square-pyramidal structure adopted by the nickel– and magnesium–trimethylarsine oxide complexes is closely similar to that reported for $[Co(Ph_2MeAsO)_4ClO_4]ClO_4$.[2] In addition other studies[1,3] have indicated the existence of the same basic geometry in other arsine oxide– and phosphine oxide–metal systems. The availability of data for both a transition metal ion complex and a regular element complex having closely similar structures provides some insight as to why the square-pyramidal structure is favored. Also, these data highlight differences in the axial and basal plane binding of the ligands.

(1) Stabilization of the Square Pyramidal Structure. A striking feature of the observed structure is the closeness of the basal arsenic atoms to the mean plane of the $(OAs)_4$ grouping (Table VIII). This produces a square-pyramidal structure which has a large cavity opposite the axial group. Although there is a reasonably close intercationic contact between the metal atom and a methyl group from a neighboring cation (M···C ≥ 3.8 Å), it is unlikely that the particular square-pyramidal structure observed results from crystal-packing forces. Indeed electronic spectra show that square-pyramidal $[Ni(Me_3AsO)_5]^{2+}$ can exist as a stable entity in solution.[3] A similar but not so pronounced effect has been observed for the structure of $[Mn(Ph_3PO)_4I]^+$.[20] Similarly in the structure of $[Co(Ph_2MeAsO)_4ClO_4]ClO_4$[2] the same essentially planar $(OAs)_4$ geometry is found even though the steric requirements of the Ph_2MeAsO ligand are quite different from those of Me_3AsO.

It has usually been assumed that for high-spin complexes (such as this nickel complex) five-coordination is stabilized primarily by particular steric properties of the ligands.[8,21,22] However, if this was the case for R_3XO oxo complexes, a different molecular structure from that observed might have been expected. Steric interactions would possibly favor the trigonal-bipyramidal structure as found for the high-spin ML_5 complex $[Co(2\text{-picO})_5]^{2+}$ [23] (2-picO = 2-picoline *N*-oxide). Also, in these cations, rotation of Me_3As groups of the basal ligands (about M–O bonds) away from the axial group would appear to give a more sterically favorable structure.

It is apparent that these structures are stabilized by some factor(s) in addition to M–O σ bonding. To a first approximation this effect must be independent of the stabilizing effect of a partially filled d shell of the central metal atom as essentially the same geometrical arrangement is adopted by Mg^{2+} and Ni^{2+}. The M–O–As bond angles for the basal plane

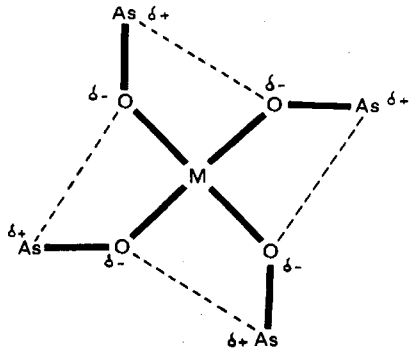

Figure 4. Interactions of oxygen atoms with arsenic atoms of adjacent ligands.

are significantly smaller than for the less hindered axial ligand and smaller than found for other arsine oxide complexes.[24,25] The observed basal M–O–As angle (~127°) produces a relatively close approach between arsenic and oxygen atoms of adjacent ligands (~3.1 Å). In addition the value indicates close to sp^2 hybridization for the oxygen atom and favorable disposition of the oxygen lone pair toward an arsenic atom of a neighboring ligand. We suggest one stabilizing influence could be an electrostatic-type interaction between neighboring oxygen and arsenic atoms as illustrated in Figure 4. This type of interaction could prevent free rotation of the Me_3As groups about the M–O bond. However the basically planar ML_4 structure may be stabilized by several interligand interactions including favorable steric packing of the arsenic methyl groupings.

(2) Comparison of the Nickel and Magnesium Structures. The ionic radii of Ni^{2+} and Mg^{2+} are closely similar (0.69 and 0.65 Å, respectively).[26] A comparison of structural parameters, for the two molecules should therefore give a good indication of the influence of the partially filled d shell in the case of Ni^{2+}.

From Tables VI–VIII it can be seen that differences between the two structures are generally small and in only a few instances greater than the standard deviation values. However there are general and consistent trends indicating (a) marginally stronger "basal" metal–ligand bonding for nickel and (b) marginally stronger "axial" bonding for magnesium.

(a) Although the ionic radius of nickel is slightly greater than that for magnesium, Ni–O "basal" distances are not longer than those for Mg–O and possibly marginally shorter. Also the nickel atom is more closely coplanar with the $(OAs)_4$ grouping than magnesium, indicating greater metal–ligand π bonding[20] (Table VIII). This difference is also indicated by the O(1)–M–O(3) and O(2)–M–O(4) angles which differ significantly for the two structures (in both cases they are greater for M = Ni).

Table VI. Selected Interatomic Distances (Å) in $[M(Me_3AsO)_5](ClO_4)_2$

	M = Ni	M = Mg
	Cation	
M–O(1)	2.00 (1)	2.049 (9)
M–O(2)	2.00 (1)	2.017 (9)
M–O(3)	2.00 (1)	2.03 (1)
M–O(4)	2.01 (1)	2.010 (9)
Av	2.00 (1)[a]	2.03 (2)
M–O(5)	1.94 (2)	1.92 (1)
As(1)–O(1)	1.68 (1)	1.668 (8)
As(2)–O(2)	1.67 (1)	1.670 (8)
As(3)–O(3)	1.65 (1)	1.641 (9)
As(4)–O(4)	1.66 (1)	1.688 (8)
Av	1.67 (1)	1.67 (2)
As(5)–O(5)	1.63 (2)	1.65 (1)
M···As(1)	3.263 (4)	3.313 (4)
M···As(2)	3.289 (4)	3.318 (4)
M···As(3)	3.292 (4)	3.329 (4)
M···As(4)	3.276 (4)	3.311 (4)
M···As(5)	3.492 (4)	3.536 (4)
As(1)···O(2)	3.11 (1)	3.166 (8)
As(2)···O(3)	3.11 (1)	3.155 (9)
As(3)···O(4)	3.05 (1)	3.082 (8)
As(4)···O(1)	3.05 (1)	3.078 (8)
As(1)–C(11)	1.94 (2)	1.90 (2)
As(1)–C(12)	1.92 (2)	1.92 (2)
As(1)–C(13)	1.88 (2)	1.91 (2)
As(2)–C(21)	1.95 (2)	1.93 (2)
As(2)–C(22)	1.94 (2)	1.93 (1)
As(2)–C(23)	1.88 (3)	1.94 (1)
As(3)–C(31)	1.96 (3)	1.94 (2)
As(3)–C(32)	1.91 (2)	1.94 (2)
As(3)–C(33)	1.95 (3)	1.90 (2)
As(4)–C(41)	1.92 (2)	1.90 (1)
As(4)–C(42)	1.97 (2)	1.95 (1)
As(4)–C(43)	1.96 (2)	1.94 (1)
As(5)–C(51)	1.93 (3)	1.90 (2)
As(5)–C(52)	1.90 (3)	1.85 (2)
As(5)–C(53)	1.87 (3)	1.86 (2)
	Anion	
Cl(1)–O(11)	1.32 (2)	1.35 (2)
Cl(1)–O(12)	1.31 (2)	1.33 (2)
Cl(1)–O(13)	1.23 (2)	1.23 (2)
Cl(1)–O(14)	1.31 (3)	1.35 (2)
Cl(2)–O(21)	1.29 (3)	1.31 (2)
Cl(2)–O(22)	1.38 (2)	1.36 (2)
Cl(2)–O(23)	1.28 (2)	1.32 (2)
Cl(2)–O(24)	1.29 (3)	1.33 (3)

[a] Esd's for average bond lengths were calculated from the expression $\sigma = \Sigma_{i=1}^{i=N}[(l_i - \bar{l})^2/(N-1)]^{1/2}$, where l_i is the ith bond length and $\bar{l}$ is the averaged bond length.

(b) While there is no significant difference in the M–O "axial" values, the M–O(5)–As(5) angle associated with this grouping is about 7° greater for the magnesium complex. This may indicate stronger bonding for magnesium, resulting from enhanced M←L (axial) π bonding. For both complexes the M–O–As (axial) angle is considerably larger than that for the basal ligands (~160° compared with ~127°). This together with the shorter axial M–O bond lengths (~1.9 Å compared with ~2.0 Å) indicates greater s character for the axial oxygen hybrid orbitals and the possibility that M←L (axial) π bonding may be important. Any π bonding involving metal dπ and *two* oxygen pπ orbitals would produce larger M–O–As bond angles.

The differences summarized in paragraphs (a) and (b) may be rationalized in terms of the electronic configurations of nickel and magnesium. While the involvement of empty 3d orbitals in bonding to magnesium would not normally be considered, the energy-lowering effect of the electronegative oxygen environment could enable dπ←pπ (axial) bonding to occur. Such bonding would be expected to be greater for a metal ion with *empty* 3d orbitals (like magnesium) compared with one like nickel having a partially filled 3d shell. The observations mentioned in paragraph (b) appear to support this conclusion. By contrast the evidence for stronger metal–ligand basal π bonding for nickel may be understood in terms of metal→ligand π donation which would be expected to be greater for the ion having the greater number of d electrons (nickel ($3d^8$) > magnesium ($3d^0$)).

While there are uncertainties about the exact nature of the M→L π bonding, evidence for electronic influence from the penultimate (P or As) atom in metal–oxo (R_3XO, X = P, As) bonding has been obtained from electronic spectra of a range of cobalt complexes.[27]

Note Added in Proof. A short "nonbonded" interaction between oxygen and tetrahedral arsenic atoms, of the same ~3.1 Å value found for the structures reported here, has recently been determined for a substituted triphenylarsonium cyclopentadienylide ion.[28]

Table VII. Selected Bond Angles (deg) in $[M(Me_3AsO)_5](ClO_4)_2$ (Cation)

	M = Ni	M = Mg
M–O(1)–As(1)	124.6 (8)	125.8 (5)
M–O(2)–As(2)	127.4 (7)	128.0 (5)
M–O(3)–As(3)	128.2 (8)	129.6 (5)
M–O(4)–As(4)	126.6 (8)	126.9 (5)
M–O(5)–As(5)	157 (1)	163.8 (8)
O(5)–M–O(1)	96.6 (7)	98.6 (5)
O(5)–M–O(2)	102.1 (7)	106.4 (5)
O(5)–M–O(3)	100.3 (7)	101.0 (5)
O(5)–M–O(4)	105.9 (8)	108.9 (5)
O(1)–M–O(2)	87.2 (5)	86.7 (4)
O(2)–M–O(3)	89.1 (5)	88.3 (4)
O(3)–M–O(4)	88.1 (6)	86.4 (4)
O(4)–M–O(1)	87.5 (6)	86.8 (4)
O(1)–M–O(3)	163.1 (6)	160.4 (5)
O(2)–M–O(4)	151.9 (6)	144.7 (5)

Table VIII. Reference Least-Squares Planes for $[M(Me_3AsO)_5]^{2+}$ cations[a]

	Distance of atom from plane/Å	
	Plane I (M = Ni)	Plane II (M = Mg)
For Atoms Included in Least-Squares Planes		
As(1)	0.223 (3)	0.232 (3)
As(2)	−0.080 (3)	−0.119 (3)
As(3)	0.047 (3)	0.099 (3)
As(4)	−0.069 (3)	−0.115 (3)
O(1)	−0.07 (1)	0.00 (1)
O(2)	−0.18 (1)	−0.19 (1)
O(3)	0.20 (2)	0.21 (1)
O(4)	−0.08 (2)	−0.12 (1)
For Other Atoms		
M	0.359 (3)	0.454 (3)
As(5)	3.844 (3)	3.985 (3)
C(12)	0.38 (3)	0.40 (2)
C(22)	−0.42 (3)	−0.43 (2)
C(32)	0.09 (3)	0.17 (3)
C(42)	−0.04 (3)	−0.11 (2)

[a] Equations of planes referred to orthorhombic crystallographic axes X, Y, Z are atomic coordinates in Å: (I) $0.0382X + 0.9992Y - 0.0105Z = 2.6188$; (II) $0.0276X + 0.9996Y - 0.0020Z = 2.6408$.

Registry No. $[Ni(Me_3AsO)_5](ClO_4)_2$, 21508-99-6; $[Mg(Me_3AsO)_5](ClO_4)_2$, 57033-84-8.

Supplementary Material Available: Structure factor tables (18 pages). Ordering information is given on any current masthead page.

References and Notes

(1) J. Lewis, R. S. Nyholm, and G. A. Rodley, *Nature (London)*, **207**, 72 (1965).
(2) P. Pauling, G. B. Robertson, and G. A. Rodley, *Nature (London)*, **207**, 73 (1965).
(3) A. M. Brodie, S. H. Hunter, G. A. Rodley, and C. J. Wilkins, *Inorg. Chim. Acta*, **2**, 195 (1968).
(4) S. H. Hunter, R. S. Nyholm, and G. A. Rodley, *Inorg. Chim. Acta*, **3**, 631 (1969).
(5) D. M. L. Goodgame, M. Goodgame, and P. J. Hayward, *J. Chem. Soc. A*, 1352 (1970).
(6) F. Mani, *Inorg. Nucl. Chem. Lett.*, **7**, 447 (1971).
(7) M. W. G. de Bolster, I. E. Kortram, and W. L. Groeneveld, *J. Inorg. Nucl. Chem.*, **34**, 575 (1972).
(8) S. H. Hunter, K. Emerson, and G. A. Rodley, *Chem. Commun.*, 1398 (1969).
(9) G. B. Jameson and G. A. Rodley, *Inorg. Nucl. Chem. Lett.*, **11**, 547 (1975).
(10) R. Timkovich and A. Tulinsky, *J. Am. Chem. Soc.*, **91**, 4430 (1969).
(11) K. Ballschmiter and J. J. Katz, *J. Am. Chem. Soc.*, **91**, 2661 (1969).
(12) S. H. Hunter, Ph.D. Thesis, University of Canterbury, 1970.
(13) "International Tables for X-Ray Crystallography", Vol. III, Kynoch Press, Birmingham, England, 1962.
(14) Calculations were carried out at the University of Canterbury using a Burroughs B6718 computer. The data processing program HILGOUT is based on programs DRED (J. F. Blount) and PICKOUT (R. J. Doedens). Numerical absorption corrections are applied using program DABS which is a modified version of DATAPH (P. Coppens).
(15) Structure factor calculations and least-squares refinements were carried out using program CUCLS and Fourier summations using program FOURIER. These are highly modified versions of the well-known programs ORFLS (W. R. Busing, K. O. Martin, and H. A. Levy) and FORDAP (A. Zalkin), respectively. Other programs include local modifications of Busing and Levy's ORFFE function and error program, and Johnson's ORTEP thermal ellipsoid plotting program.
(16) D. T. Cromer and J. B. Mann, *Acta Crystallogr., Sect. A*, **24**, 321 (1968).
(17) R. F. Stewart, E. R. Davidson, and W. T. Simpson, *J. Chem. Phys.*, **42**, 3175 (1965).
(18) D. T. Cromer, *Acta Crystallogr.*, **18**, 17 (1965).
(19) M. J. Buerger, "Vector Space", Wiley, New York, N.Y., 1959, p 66.
(20) G. Ciani, M. Manassero, and M. Sansori, *J. Inorg. Nucl. Chem.*, **34**, 1760 (1972).
(21) J. S. Wood, *Prog. Inorg. Chem.*, **16**, 227 (1965).
(22) R. Morassi, I. Bertini, and L. Sacconi, *Coord. Chem. Rev.*, **11**, 343 (1973).
(23) B. A. Coyle and J. A. Ibers, *Inorg. Chem.*, **9**, 767 (1970).
(24) I. Lindquist, "Inorganic Adduct Molecules of Oxo-Compounds", Springer-Verlag, Berlin, 1963, p 69.
(25) C. I. Branden, *Acta Chem. Scand.*, **17**, 1363 (1963).
(26) F. A. Cotton and G. Wilkinson, "Advanced Inorganic Chemistry", Wiley, New York, N.Y., 1972, p 52.
(27) A. M. Brodie, S. H. Hunter, G. A. Rodley, and C. J. Wilkins, *J. Chem. Soc. A*, 2039 (1968).
(28) F. C. March, G. Ferguson, and D. Lloyd, *J. Chem. Soc., Dalton Trans.*, 1377 (1975).

Contribution from the Department of Chemistry, Arizona State University, Tempe, Arizona 85281

Crystal and Molecular Structure of Tetraisothiocyanatobis(2,2'-bipyridine)niobium(IV) and -zirconium(IV)

E. J. PETERSON, R. B. VON DREELE, and T. M. BROWN*

Received April 8, 1975 AIC502570

The crystal and molecular structures of the eight-coordinate complexes $Nb(NCS)_4(C_{10}H_8N_2)_2$ and $Zr(NCS)_4(C_{10}H_8N_2)_2$ have been determined from single-crystal x-ray intensity data collected by the θ–2θ scan technique. In both compounds the metal atoms are coordinated by eight nitrogen atoms, four belonging to the two bidentate 2,2'-bipyridine groups and four belonging to the isothiocyanate ligands. The niobium–nitrogen distances are 2.135 (3) and 2.318 (3) Å, respectively, for the M–NCS and M–2,2'-bpy bonds, while the zirconium–nitrogen distances are 2.182 (2) and 2.412 (2) Å, respectively. The coordination geometries around the metal for both complexes can be obtained by distortions from an idealized D_{2d} dodecahedron along a reaction pathway which retains D_2 symmetry. The degree of distortion correlates with the M–N bond lengths; the smaller niobium complex is sufficiently distorted from a dodecahedron to become a very nearly perfect D_4 square antiprism ($\delta = -2.1, 49.2°$) with the bidentate 2,2'-bipyridines bridging the square faces. The larger zirconium complex is significantly less distorted ($\delta = 4.2, 45.5°$) from the D_{2d} dodecahedron than the niobium complex. Each structure was solved by standard heavy-atom techniques and refined by full-matrix least-squares to final R values of 0.067 (1702 independent observed reflections) for $Nb(NCS)_4(C_{10}H_8N_2)_2$ and 0.056 (1833 independent observed reflections) for $Zr(NCS)_4(C_{10}H_8N_2)_2$. Both compounds crystallize in the orthorhombic space group $Pnnn$, $Z = 2$, with the lattice parameters $a = 7.720$ (4), $b = 13.179$ (7), $c = 13.113$ (4) Å for $Nb(NCS)_4(C_{10}H_8N_2)_2$ and $a = 7.646$ (6), $b = 13.407$ (11), $c = 13.245$ (11) Å for $Zr(NCS)_4(C_{10}H_8N_2)_2$.

Introduction

The elucidation of factors which govern the stereochemistry of eight-coordinate compounds has been the subject of a number of papers.[1-8] Some examples of discrete eight-coordinate complexes and their experimentally assigned stereochemistries are listed in Table I. In general, eight-coordinate complexes are usually classified as either a D_{2d}-$\bar{4}2m$ dodecahedron or a D_{4d}-$\bar{8}2m$ square antiprism. Recently, however, several authors have expressed consternation because many of the usual polyhedron-shape criteria neglect the possibility of a C_{2v} bicapped trigonal prism. Because of these objections, new criteria were proposed which relate the three most common polyhedra along a geometric reaction pathway.[7,8] Several theoretical studies have shown that both the D_{2d} and D_{4d} stereochemistries are equally likely on the basis of crystal field stabilization[3] or minimization of repulsions.[1,3,6] The MX_8 and MX_4Y_4 systems show predominantly dodecahedral stereochemistry, while the $M(A–A)_4$ compounds are divided between dodecahedral and square-antiprismatic structures. The latter observations have been explained in terms of the normalized ligand bite of the symmetrical bidentate ligands.[6] The structure of $Nb[(t\text{-}C_4H_9CO)_2CH]_4$ was recently investigated and found to be a distorted D_4 square antiprism.[9] This structure is significant because it is the first $M(A–A)_4$ system where the bidentate ligands span the l edges of an idealized antiprism.

Eight-coordinate complexes of the type $M(A–A)_2B_4$ are also of interest but have not been as extensively studied as the other systems. Most reported examples are dodecahedral and only a few compounds of this type which even closely approach a square antiprism have been reported, i.e., $W(CH_3)_4[O\text{-}N(CH_3)NO]_2$[10] and $Zr(SO_4)_2\cdot 4H_2O$.[11] Thus, in order to elucidate further the factors governing the stereochemical arrangement of ligands in eight-coordinate complexes,